

Chemolithoautotrophic production mediating the cycling of the greenhouse gases N_2O and CH_4 in an upwelling ecosystem

L. Farías¹, C. Fernández^{1,2}, J. Faúndez¹, M. Cornejo¹, and M. E. Alcaman¹

¹Laboratorio de Procesos Oceanográficos y Clima (PROFC), Departamento de Oceanografía and Centro de Investigación Oceanográfica en el Pacífico Suroriental (COPAS, Universidad de Concepción, Casilla 160-C, Concepción, Chile

²Laboratoire d'Océanographie biologique de Banyuls, Université Paris VI, CNRS-UMR 7621, BP44, 66651 Banyuls-sur-Mer Cedex, France

Received: 19 May 2009 – Published in Biogeosciences Discuss.: 30 June 2009

Revised: 29 October 2009 – Accepted: 4 November 2009 – Published: 17 December 2009

Abstract. The high availability of electron donors occurring in coastal upwelling ecosystems with marked oxyclines favours chemoautotrophy, in turn leading to high N_2O and CH_4 cycling associated with aerobic NH_4^+ (AAO) and CH_4 oxidation (AMO). This is the case of the highly productive coastal upwelling area off central Chile (36°S), where we evaluated the importance of total chemolithoautotrophic vs. photoautotrophic production, the specific contributions of AAO and AMO to chemosynthesis and their role in gas cycling. Chemolithoautotrophy was studied at a time-series station during monthly (2007–2009) and seasonal cruises (January 2008, September 2008, January 2009) and was assessed in terms of the natural C isotopic ratio of particulate organic carbon ($\delta^{13}\text{C}_{\text{POC}}$), total and specific (associated with AAO and AMO) dark carbon assimilation (CA), and N_2O and CH_4 cycling experiments. At the oxycline, $\delta^{13}\text{C}_{\text{POC}}$ averaged -22.2‰ ; this was significantly lighter compared to the surface (-19.7‰) and bottom layers (-20.7‰). Total integrated dark CA in the whole water column fluctuated between 19.4 and $2.924\text{ mg C m}^{-2}\text{ d}^{-1}$, was higher during active upwelling, and contributed 0.7 to 49.7% of the total integrated autotrophic CA (photo plus chemoautotrophy), which ranged from 135 to $7.626\text{ mg C m}^{-2}\text{ d}^{-1}$, and averaged 20.3% for the whole sampling period. Dark CA was reduced by 27 to 48% after adding a specific AAO inhibitor (ATU) and by 24 to 76% with GC7, a specific archaea inhibitor. This indicates that AAO and AMO microbes (most of them archaea) were performing dark CA through the oxidation of NH_4^+ and CH_4 . Net N_2O cycling rates varied between 8.88 and 43 nM d^{-1} , whereas net CH_4 cycling rates ranged from

-0.41 to -26.8 nM d^{-1} . The addition of both ATU and GC7 reduced N_2O accumulation and increased CH_4 consumption, suggesting that AAO and AMO were responsible, in part, for the cycling of these gases. These findings show that chemically driven chemolithoautotrophy (with NH_4^+ and CH_4 acting as electron donors) could be more important than previously thought in upwelling ecosystems, raising new questions concerning its relevance in the future ocean.

1 Introduction

Coastal upwelling regions, most of which are associated with eastern boundary current systems, significantly influence oceanic biogeochemistry in terms of marine productivity and atmospheric chemistry. Although they represent less than 1% of the area of the ocean, these regions provide about 20% of the global fish catch (Pauly and Chistensen, 1995) and give off intense N_2O and CH_4 emissions (Law and Owens, 1990; Owens et al., 1991; Nevinson et al., 2004). Physical forcing (through favourable wind stress) generally explains most biological production (Rykaczewski and Checkley, 2008), bringing nutrient-rich water from below the pycnocline to the surface layer, thereby boosting phytoplankton production. The supply of nutrients to the surface in terms of new nitrogen (NO_3^-) results in high organic matter or “new” production (Eppley, 1989).

The formation of planktonic biomass in such highly productive marine areas also results in O_2 consumption, as organic matter (OM) respiration takes place throughout the water column. O_2 gradients or oxyclines act as a chemical forcing (or redox gradient) for micro-organisms and, therefore, for important biogeochemical processes (Pimenov and Neretin, 2006). NH_4^+ is released during organic matter



Correspondence to: L. Farías
(lfarias@profc.udec.cl)

decomposition, whereas NO_2^- , HS^- , and CH_4 are produced if NO_3^- , SO_4^{2-} , and CO_2 are used as electron acceptors for anaerobic organic matter respiration. Thus, although NH_4^+ , NO_2^- , HS^- , and other compounds can encounter different fates, they are most likely to be used as electron donors for the chemolithoautotrophic microbes processing carbon (C) in dark conditions. Although the presence of dark CO_2 assimilation or chemolithoautotrophic activity has been observed in a variety of marine environments associated with redoxclines such as the Cariaco Basin (Taylor et al., 2001), the Black Sea (Pimelov and Neretin, 2006), the Baltic Sea (Jost et al., 2008), fjords (Zopfi et al., 2001), and hydrothermal vents (both in free and episymbiotic micro-organisms; Lein et al., 1997; Campbell et al., 2003), such activity has not been examined sufficiently in highly productive coastal upwelling ecosystems.

Among chemolithoautotrophic microorganisms, nitrifying bacterioplankton (namely aerobic NH_4^+ and NO_2^- oxidizers, AAO and ANO, respectively) transform NH_4^+ and NO_2^- to NO_3^- as a means of securing the reducing power to synthesize organic matter from CO_2 (Ward et al., 1989). Methanotrophic micro-organisms are distinguished by their ability to use CH_4 as their reducing power and sole source of carbon (Schubert et al., 2006). Both NH_4^+ and CH_4 -oxidizing microbes are obligate aerobic chemolithoautotrophs. They play a central role in the biogeochemical cycles of carbon and nitrogen because they produce organic matter but also because they can recycle bio-elements such as the greenhouse gases N_2O and CH_4 , both of which participate in the depletion of stratospheric ozone through photochemical reactions (Crutzen, 1991). These trace gases contribute about 6% and 15% to the global greenhouse effect, respectively (IPCC, 2007).

The cycling of N_2O involves processes that produce and consume it. N_2O is mainly produced by nitrification through aerobic ammonium oxidation (Codispoti and Christensen, 1985) but some species of nitrifying bacteria can produce N_2O by reducing nitrite through a process called nitrifier denitrification (Arp and Stein, 2003). Furthermore, dissimilatory nitrite reduction (called partial denitrification; Codispoti and Christensen, 1985) or dissimilatory nitrate reduction to ammonium (DNRA) could be a relatively important N_2O producing process (Kartal et al., 2007). However, the complete N-oxide (e.g., NO_3^-) reduction to N_2 is the only reaction able to consume N_2O (Elkin et al., 1978; Farias et al., 2009). It is important to note that N_2O is not an intermediate of anaerobic ammonium oxidation (anammox), although it is known that, at very low relative percentages, NO detoxification by anammox and other bacteria could be a potential source of N_2O .

The cycling of CH_4 also involves producing and consuming processes. Methanogens (CH_4 -producing bacteria) can use a range of substrates, including CO_2 , formate, and acetate to generate CH_4 during anaerobic respiration

of organic matter, so methanogenesis occurs in anoxic environments. In contrast, two processes have been reported to consume CH_4 : aerobic and anaerobic CH_4 oxidation. During the first reaction, O_2 is the electron acceptor. For the second reaction, SO_4^{2-} or NO_3^- can be used (Valentine and Reeburgh, 2003). Whereas anaerobic methane oxidation is mediated by a consortium of CH_4 -consuming archaea and sulphate-reducing proteobacteria (Schubert et al., 2006), in the presence of O_2 , aerobic CH_4 oxidation prevails.

The coastal ecosystem off central Chile presents intense upwelling in austral spring and summer (70% of the year) due to favourable wind stress (Cornejo et al., 2007). The seasonal intensification of the south and southwest winds brings Equatorial Subsurface Water (ESSW), with high NO_3^- and low O_2 concentrations, to the surface (Sobarzo and Djurfeldt, 2004). The width of the continental shelf provides a large surface area for material exchange and benthic-pelagic coupling in subsurface waters that can reach the surface via upwelling processes. The most significant consequences of this coastal upwelling are the fertilization of the photic zone, which sustains high primary production ($3\text{--}20\text{ g C m}^{-2}\text{ d}^{-1}$, Daneri et al., 2000; Farías et al., 2004) and the outgassing of N_2O (Cornejo et al., 2007). In late autumn and early winter, however, Sub-Antarctic Water (SAAW), high in dissolved O_2 and low in nutrients, occupies the uppermost part of the water column and northerly winds predominate, driving strong, efficient vertical mixing of the water column. In this period, the coastal area acts as a N_2O sink (Cornejo et al., 2007).

This area has shallow, intense O_2 (oxycline) and nutrient (nutricline) gradients. The presence of O_2 -poor waters generates an O_2 and electron donor downward flux (associated with the active breakdown of organic matter produced in the surface layer). Also, the intense mineralization of organic matter produced in the water and sediment generates an upward flux of electron donors such as HS^- , CH_4 , and NH_4^+ , offering a substantial substrate for the existence of autotrophic mechanisms – other than photosynthetic – in the water column. These, in turn, drive intense nutrient and gas cycles.

This study explores the existence of important alternative autotrophic processes acting in the C and N cycling of the continental shelf waters off central Chile: aerobic ammonium and methane oxidizing pathways. By evaluating these chemolithoautotrophic processes, we will attempt to answer the following questions: what is the relative importance of chemo- vs. photo-autotrophic production? Are nitrifying and methanotrophic activities significantly involved in dark C assimilation? Are AAO and AMO responsible for N_2O and CH_4 cycling in the coastal upwelling area off central Chile, and do they influence the gas exchange across the air-sea interface (i.e., AAO favours N_2O effluxes whereas AMO reduces CH_4 effluxes into the atmosphere).

2 Materials and methods

2.1 Site description and sampling strategy

Field work was carried out at the time-series station 18 ($36^{\circ}30.8' S$; $73^{\circ}07.75' W$), located 18 nautical miles from the coast (92 m depth) over the widest continental shelf of Chile (ca. 3.066 km^2), between the Bio Bio and Itata submarine canyons (Fig. 1). Monthly cruises (L/C Kay-Kay, Universidad de Concepción) have been carried out at Station 18 since August 2002 as part of the time-series program of the Centre for Oceanographic Research in the eastern South Pacific (COPAS) in order to identify physical and biological variability in this upwelling ecosystem. Hydrographic data (temperature, salinity, O_2 , fluorescence, light) were obtained from the water column using a CTD- O_2 probe (Seabird 25). An optical sensor (Satlantic) was attached to the CTD. Water samples were collected at 2, 5, 10, 15, 20, 30, 40, 50, 65, and 80 m depth (and sometimes at 90 m) using Niskin bottles (10 L) attached to a rosette sampler. Gas (O_2 and N_2O) and nutrient (NH_4^+ , NO_3^- , NO_2^- , and PO_4^{3-}) measurements were routinely performed. In situ autotrophic carbon assimilation rates and CH_4 measurements were included in this program in early 2007. The determination of natural abundances of C isotopes in POC started in late 2007.

In addition to the ongoing time-series program, three seasonal process-oriented cruises were performed in order to assess specific pathways of chemoautotrophic processes: NICCHEX I (January 2008) and MI-LOCO I (January 2009) in upwelling periods and NICCHEX II (September 2008) in a non-upwelling period. During these cruises, water samples were taken from the oxycline (set at 30 m depth) and near-bottom water (80 m depth, in order to avoid the effect of particulate organic matter re-suspension) for biological incubations. The samples were used for light and dark C assimilation and N_2O and CH_4 time course experiments.

2.2 Field measurements

2.2.1 Chemical and geochemical analyses

During this study, samples for gas analysis were taken in triplicate. Dissolved O_2 (125 mL sample) was analyzed with an automatic Winkler method (AULOX Measurement System) developed at PROF-C-Universidad de Concepción. N_2O (20 mL sample) was analyzed by creating 5 mL He headspace and equilibration in the vial, and then quantifying the N_2O with a gas chromatograph (Varian 3380) using an electron capture detector maintained at $350^{\circ}C$ and connected to an autosampler device (for more details, see Cornejo et al., 2007). CH_4 (20 mL sample) was manually analyzed on a gas chromatograph with Flame ionization detector (Schimadzu 17A) through a capillary column GS-Q (J&W, $0.53 \text{ mm} \times 30 \text{ m}$) with $30^{\circ}C$ oven temperature and

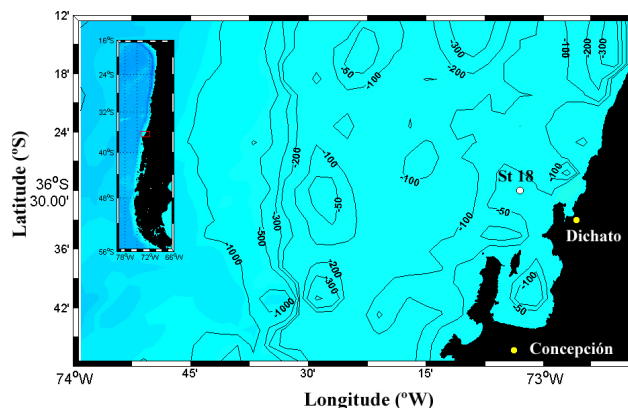


Fig. 1. Map showing the location of Station18 ($36^{\circ}30.80' S$; $73^{\circ}07.75' W$), occupied monthly by the COPAS oceanographic centre for a physical-chemical-biological integrated time-series study since August 2002. Central Chile's continental shelf is delimited to the north and south by two submarine canyons. Bathymetric contours are in metres.

4 ml min^{-1} column flow. Previously, the seawater sample was equilibrated to $40^{\circ}C$ within 5 mL He headspace.

Dissolved NH_4^+ was determined immediately after sampling, whereas samples for dissolved NO_2^- , NO_3^- , and PO_4^{3-} were filtered ($0.7 \mu\text{m}$, type GF-F glass filter) on board and stored frozen until analysis. Concentrations of NO_2^- , NO_3^- , and PO_4^{3-} were determined using standard manual colourimetric techniques following Grasshoff et al. (1983). The precision of NO_3^- and NO_2^- , in terms of coefficient variation, was better than $\pm 10\%$ and $\pm 3\%$, respectively. For NH_4^+ concentrations, samples (triplicate) were taken directly from the Niskin bottle in 50-mL Pyrex (Duran Schott) flasks. Each sample (40 mL) received 10 mL of working solution (OPA). Samples were then stored in the dark for 2 h and analyzed by the fluorometric method (Holmes et al., 1999) using a Turner design fluorometre. The standard error of this technique was lower than $\pm 5\%$.

2.2.2 In situ carbon assimilation (CA) rates and natural C isotopic ratio for POC

Monthly rates of light and dark CA (representing total photoautotrophic and chemoautolithotrophic production, respectively) were obtained through incubations using the ^{13}C stable isotopic technique on an in situ mooring line. Samples from different depths were labeled with ^{13}C in the form of $NaH^{13}CO_3$ (99% ^{13}C). The tracer was added at a final tracer concentration of 10% final enrichment (0.5 for 580 mL incubation volume). The incubations lasted ca. 10 h (samples were generally taken at dawn and put on the line before sunrise) and were terminated by filtration through pre-combusted $0.7\text{-}\mu\text{m}$ glass fibre filters (12 h; $450^{\circ}C$). Filters were dried at $60^{\circ}C$ for 24 h and then

stored at a constant temperature until laboratory analysis by continuous-flow isotope ratio mass spectrometry (IRMS, Finnigan Delta Plus). Prior to the analysis, samples were acid-fumed to remove carbonates. International standard reference material was used for all analyses (Acetanilide).

For the elemental analysis of C and N contents in particulate organic matter and natural ^{13}C isotopic characterization, 1 L of seawater per depth was filtered through precombusted $0.7\ \mu\text{m}$ glass fibre filters (type Whatman GF-F). IRMS sample analysis was performed as specified above. Reproducibility for ^{13}C (based on standards) was better than 0.11‰. Isotope ratios were expressed as per mil deviations of the isotopic composition of Vienna PDB, the internationally accepted standard, as defined by Eq. (1):

$$\delta^{13}\text{C}(\text{‰}) = [R_{\text{Sample}}/R_{\text{Standard}} - 1] \times 1000 \quad (1)$$

where $R = {}^{13}\text{C}:{}^{12}\text{C}$.

Light and dark CA rates were calculated following Slawyk and Collos (1984), as stated in Eqs. (2) and (3):

$$\rho\text{DI}^{13}\text{C} = \left[\frac{(\%R_{\text{POC}} - R_n) * \left(\frac{\text{POC}}{12 * V_f} \right)}{\%R_{\text{DIC}}} \right] * 12 \quad (2)$$

$$\%R_{\text{DIC}} = \frac{\left(\frac{V^{13}\text{C}_i * {}^{13}\text{C}_{\text{DIC}}}{V_b} \right) + \text{DIC}_i * 0.01112}{\text{DIC}_i - \frac{V^{13}\text{C}_i * {}^{13}\text{C}_{\text{DIC}}}{V_b}} * 100 \quad (3)$$

where V_f represents the filtered volume and POC is the amount of particulate organic carbon recovered on the filter after incubation and measured by mass spectrometry (μg). The excess enrichment of the tracer after inoculation (T_o) is indicated by $\%R_{\text{DIC}}$, which is calculated using Eq. (3). The $\%R_{\text{POC}}$ indicates the ^{13}C enrichment on the filter after incubation, measured by the tracer mass. In Eq. (3), $V^{13}\text{C}$ indicates the volume of ^{13}C added to the sample during inoculation, whereas $^{13}\text{C}_{\text{DIC}}$ refers to the tracer concentration added to the sample ($3.6456\ \text{mg } ^{13}\text{C ml}^{-1}$). DIC_i represents the initial amount of DIC in the sample. For this study, we used a constant value ($26\ \text{mg C L}^{-1}$) based on previous DIC measurements in the study area. V_b is the volume in the incubation flask (0.6 L). Natural $\%^{13}\text{C}$ abundance in POC from August 2007 and March 2008 was used to estimate excess $\%^{13}\text{C}$ abundances in the experiment (except from April to August 2009 when an annual average of natural $\%^{13}\text{C}$ abundance in POC was considered).

In order to determine the fraction of total dark autotrophic CA that can be associated with the aerobic NH_4^+ and CH_4 oxidizing pathways, biogeochemical experiments were performed at 30 (oxycline) and 80 m depth (near-bottom water) during NICCHEX (I and II) and MI-LOCO cruises. Seawater samples were dispensed – avoiding oxygenation – into acid-cleaned 600-mL glass bottles (in duplicate or triplicate) sealed with septum caps. These were amended

with three treatments: 1) ^{13}C ; 2) ^{13}C plus allylthiourea (hereafter referred to as ATU); and 3) ^{13}C plus N1-guanyl-1,7-diaminoheptane (hereafter referred to as GC7). ATU (FLUKA), which is a specific inhibitor of the NH_4^+ monooxygenase enzyme was added at a final concentration of $86\ \mu\text{M}$ (Ginestet et al., 1998). Given the physiological and biochemical similarities between AA and AM oxidizing microbes (Hanson and Hanson, 1996), ATU may also significantly affect CH_4 cycling. GC7 (BIOSERCH), a known phylogenetic inhibitor of archaea, was added at a final concentration of 500 mM (Jansson et al., 2000) in order to inhibit the deoxyhypusine synthase enzyme. In this way, we were able to discern the group of microbes involved in CA, and in N_2O and CH_4 cycling. Experiments were incubated in the laboratory at in situ temperatures and in the dark. Incubations lasted between 13 and 24 h. Samples were filtered at three different times (t_0 , t_1 , and sometimes t_2) through pre-combusted glass fibre filters prior to mass spectrometry analysis (IRMS). Initial and final dissolved inorganic nitrogen concentrations were measured for each sample as described above.

2.2.3 N_2O and CH_4 cycling by aerobic NH_4^+ and CH_4 oxidation

During the NICCHEX and MI-LOCO cruises, experimental assays were performed in the laboratory in order to evaluate the kinetics of N_2O and CH_4 cycling and to determine possible associations with chemoautotrophic activities (e.g., AAO and AMO). For this purpose, water was dispensed – avoiding oxygenation – into 1-L double-laminated aluminium-polyethylene bags. Each bag had a hose/valve with a septum through which all the different treatments were injected. A permeability test was performed prior to the experiment. The bags were filled with helium and monitored for 24 h using gas chromatography; the lack of intrusions by atmospheric gases (N_2O or CH_4) confirmed the hermetic seal of the bags. Atmospheric oxygen could not be tested in the bags through chromatography, but oxygen intrusions were considered unlikely since N_2O was not detected inside the bag (given the sensitivity of the chromatographic method). We could then confidently exclude the possibility of oxygenation during the incubation process. The cycling rate of N_2O and CH_4 over time or its accumulation or consumption was determined under natural in situ O_2 and temperature ($11\text{--}13^\circ\text{C}$) conditions, without (the control) and with the addition of ATU and GC7 inhibitors (these were slowly injected into the bags through a septum with gastight syringes). Treatments (without any inhibitor) and poisoned treatments (with HgCl_2) were performed in order to evaluate net gas cycling (i.e., with and without biological processes that produce and consume these gases). Subsamples were retrieved from the bags for N_2O and CH_4 analysis at different times (one or two bags per experiment) by applying pressure on the bags; this water was poured into GC bottles (20 mL).

For each incubation time, three GC bottles with incubated water were injected with 50 μL of saturated HgCl_2 in order to stop all biological reactions; the bottles were then sealed with rubber stoppers and metallic caps.

The net rates of N_2O and CH_4 accumulation or consumption were calculated from the slopes of the linear regressions of the concentration as a function of time for each treatment. Positive slope values represented net gas accumulation and negative values indicated net consumption. The rate uncertainty was calculated directly from the standard error of the slope for the control, ATU, and GC7 treatments. Student's t -test and ANOVA were used to evaluate the significance of slopes and the differences between the treatments.

2.3 Data analysis

The depth of the euphotic zone (irradiation at 1% of its surface value) was estimated from the attenuation coefficient of downwelling irradiance. A density-based criterion was used to determine the mixed layer depth. In order to interpret the O_2 and electron donor vertical distributions along with CA rates, the water column was divided into three layers according to its hydrographic features: 1. an illuminated, mixed surface layer with high O_2 content; 2. a subsurface or oxycline layer layer that was always associated with the oxycline, showed hypoxic conditions and a strong redox gradient, and extended from its upper limit at the base of the euphotic zone (this nearly coincides with the mixing layer depth or the base of thermocline) to 65-m depth (this is an arbitrary depth at which O_2 levels are close to 22 μM and assumed to be uninfluenced by the sediments); and 3. a bottom layer with very low O_2 that extends from 66 m depth to the water overlying the sediments (92 m).

Integrated light and dark CA were calculated by numerically integrating (trapezoidal quadrature) the measured CA rate with respect to specific depth ranges. Integrated photosynthetic CA (light bottles) was calculated as the integrated values from the surface to the depth of 1% surface irradiance, whereas dark CA (dark bottles) were calculated by integrating rates from the surface to depth of 1% incident light (photic layer) and from 1% incident light to 92 m (aphotic layer). Hourly rates were multiplied by 12 (photo CA) or 24 (dark CA) to obtain daily rates. Gas and nutrient inventories were estimated as linear depth integrations by layer (see depth range) from interpolated data between each sampled depth. Correlations between environmental variables and geochemical parameters (nutrient and gas inventories) as well as between $\delta^{13}\text{POC}$ and CA rates were performed through Spearman rank correlation (ρ). The significance of ρ ($p < 0.05$) was determined using an F-test.

3 Results

3.1 Temporal variability of physical-chemical variables

An analysis of the vertical distribution of physical variables (including dissolved O_2) during the almost 7-year survey period allow dividing the water column into three layers, as described earlier. Figure 2 presents time-series plots (July 2002–March 2009) of temperature (T°), salinity (S), sigma- t (σt), and oxygen (O_2). These show the thermocline (11°C), halocline (34.5), pycnocline (26.5 σt), and oxycline (22 μM oxycline), all of which characterise the presence of the ESSW.

The surface layer (considered to be a well-mixed, illuminated layer whose limit is defined by the depth of the photic layer) ranged between 12 and 40 m depth and was shallower in summer than in wintertime (Table 2). The surface layer nearly coincided with the mixed layer depth, which fluctuated between 12 and 20 m depth and was influenced by the warming in summer and precipitation in winter, resulting in highly variable temperatures (11.1° < surface $T < 18.1^\circ\text{C}$; Fig. 2a) and salinity (28.73 < surface $S < 34.56$; Fig. 2b). The surface layer was always well oxygenated, with O_2 levels ranging between 329 and 183 μM (Fig. 2c).

The oxycline layer extended from the base of the surface or photic layer to 65 m depth. Although the temperature and salinity in this layer were less variable than in the surface layer, σt revealed a clear seasonal cycle (see Fig. 2d). This parameter indicated that ESSW was present almost all spring, summer and early autumn, whereas SAAW was only found in austral winter (i.e., May, June, July). Dissolved oxygen decreased abruptly in the oxycline layer, from $\sim 220 \mu\text{M}$ at the base of surface layer to ~ 2.81 at 65 m depth. The 22- μM O_2 isocline lies between 14 and 90 m but, excluding the months in which the oxycline was extremely shallow (e.g. June 2008, November 2008), the 22- μM O_2 isobaths were usually located at 60 to 70 m depth (see Fig. 2c) and, on average, at 61 m. Therefore, this confirms a good separation between the oxycline and bottom layers.

The bottom layer was confined to depths below 65 m, where the physical components were less variable (see Fig. 2 a, b, c) and the ESSW was in contact with the sediments most of the time. The O_2 content in this layer was low ($< 22 \mu\text{M}$), sometimes close to 1 to 3 μM , except in periods of strong vertical mixing (i.e., winter, see Fig. 2c). These nearly anoxic conditions were mostly observed in late summer, after several upwelling events that resulted in the accumulation of a large amount of organic matter on the sediments produced by the sedimentation of successive phytoplankton blooms.

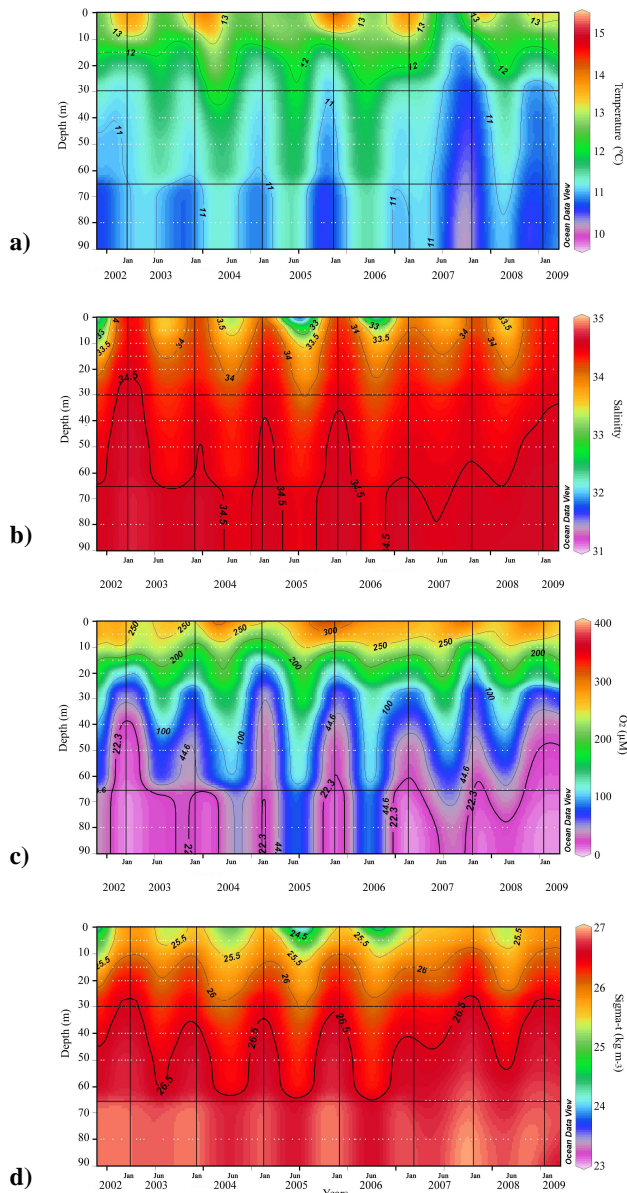


Fig. 2. Temporal variability of temperature, salinity, dissolved oxygen, and density at Station 18 (August 2002 to date). Horizontal lines separate the predetermined layers. $26.2\sigma_t$ indicates the presence of the ESSW.

3.2 Temporal variability of gases (N_2O and CH_4) and nutrients

Time-series plots for the gases N_2O and CH_4 , measured from April 2007 to March 2009, are shown in Fig. 3. The temporal variability of the N_2O content in the water column (see Fig. 3a) showed a seasonal pattern that corresponded well with the temporal O_2 variation (see Fig. 3a). In winter or non-favourable upwelling periods, the whole water column had low N_2O levels (<10 nM) but high O_2

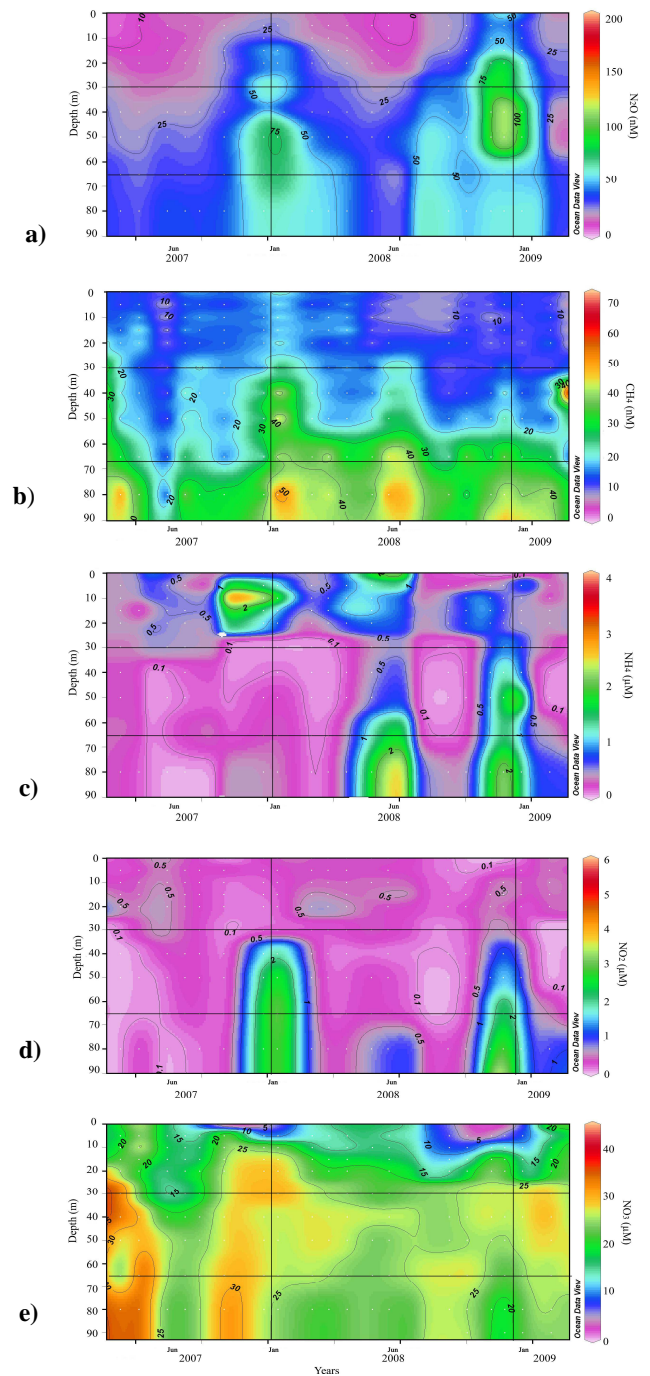


Fig. 3. Temporal variability of (a) nitrous oxide, (b) methane, (c) ammonium, (d) nitrite, and (e) nitrate concentrations at Station 18 (data from April 2007 to March 2009).

concentrations (>180 μM). In contrast, during the upwelling favourable periods, N_2O increased as O_2 decreased in the oxycline layer. Very high N_2O maxima (up to 206 nM) were observed (e.g., December 2008, January 2009) (see Fig. 3a), sometimes creating N_2O hotspots within the

oxycline layer. The temporal variability of the bottom layer was higher (20–70.6 nM), also fluctuating in relation to the O₂ fluctuations, but diminishing (sub-saturated) N₂O values were observed when the O₂ dropped below 10 μM, generally in late summer and early autumn.

The temporal variability of the vertical CH₄ distribution (see Fig. 3b) also showed seasonal variations, peaking in upwelling-favourable periods, when O₂ concentrations dropped. During these periods, the CH₄ concentration was high (up to 79.9 nM, January 2009), especially in the bottom waters, and gradually decreased towards the surface. The maximum CH₄ concentration occurred close to the seafloor, indicating that the CH₄ emission came from the sediment to the overlying water column. This vertical pattern corresponded to exponentially-decreasing O₂ concentrations and also to a marked methane production coming from the sediment and maybe even from the bottom layer. Table 1 presents N₂O and CH₄ inventories for each predefined layer. N₂O inventories were higher (on average, 42.2% of the total N₂O pool) in the oxycline layer most of the time with respect to surface and bottom layer. In contrast, CH₄ inventories indicated that most of the CH₄ was concentrated in the bottom layer (1021 μmol m⁻²), representing an average of 50% of the total CH₄ pool. The CH₄ content in the oxycline layer was lower and could sometimes be lower than values in the surface layer (see Table 1). Note that N₂O inventories did not always increase towards the sediment; the N₂O pool size in the oxycline was higher than in the surface and bottom layers in summer (up to 5.885 μmol m⁻²; see Table 1). This pattern matches the NO₃⁻ and NO₂⁻ vertical distribution (see Table 1).

Time-series plots and inventories for nutrients are shown in Fig. 3c, d, e, and Table 1, respectively. NH₄⁺ concentrations were generally high although some variability was observed. The NH₄⁺ concentrations in the surface layer varied from <0.1 to 3.5 μM (Fig. 3c, December 2007). Interestingly, this range of values is higher than the values obtained in the oxycline layer, where low concentrations were always observed. The bottom waters had the highest NH₄⁺ concentrations (up to 8.5 μM) in summer since the sediments can act as a source of NH₄⁺ (Fariás et al., 2004). On average, 25% of the total NH₄⁺ pool was present in the oxycline, whereas the surface and bottom layer contained up to 36 and 99 mmol m⁻², respectively.

Nitrite showed a marked fluctuation in the study area, ranging from 0.01 to 6.1 μM. The surface layer presented moderate and almost constant NO₂⁻ content, whereas the oxycline showed a very wide range of NO₂⁻ concentrations. This layer had a lower average NO₂⁻ inventory (27%) than the surface and bottom layer (40.4 and 32.4%, respectively). However, NO₂⁻ levels and inventories reached maxima in summer (up to 6 μM, 160 mmol m⁻²; January 2008) and were accompanied by higher N₂O and NO₃⁻ concentrations, suggesting N₂O production by AAO (see Fig. 3d, Table 1).

In the bottom water, the NO₂⁻ content was also highly variable, ranging between 0.5 and 6.1 μM (Fig. 3d). As with NH₄⁺, a fraction of the NO₂⁻ might come from the sediments, but some may also be produced by nitrification and denitrification processes that could be acting in the bottom layer under O₂ deficiency.

Nitrate concentrations were always high during our study, and the oxidized N-compound was the most abundant in the water column (see Fig. 3e). NO₃⁻ was never depleted in surface waters, not even during periods of high photoautotrophic production. Within the oxycline layer, NO₃⁻ levels were variable, ranging from 14.5 to 35.7 μM, and showed seasonal patterns, i.e., enhanced NO₃⁻ during upwelling-favourable periods and diminished NO₃⁻ during non-upwelling periods. The NO₃⁻ and N₂O inventories peaked in the oxycline during upwelling periods (December 2007 and 2008), reaching up to 1.586 mmol m⁻² and 5.885 μmol m⁻², respectively (see Table 1). The high N₂O values observed along with the higher nitrate concentrations within the oxygen gradient indicated the occurrence of NO₃⁻ regeneration and N₂O production through nitrification. In the bottom layer, NO₃⁻ concentrations decreased with respect to the NO₃⁻ values found in the oxycline layer in summer. This indicates significant NO₃⁻ consumption in the bottom water or within the sediments (e.g., March 2008, December 2008).

3.3 Carbon assimilation rates, POC content, and C isotopic composition

Temporal variations of photo and dark CA rates, POC contents, and δ¹³POC are shown in Fig. 4. Simultaneous estimations of photo and dark CA rates, POC contents, and its isotopic composition and areal daily photo and dark CA rates through photic and aphotic layers are presented in Table 2. The photo CA rate, or photoautotrophic production, varied between 0.2 and 825 mg C m⁻³ d⁻¹ and maximum rates were observed at the surface (2 m depth) during upwelling-favourable periods (December 2007, October 2008, January 2009; see Fig. 4a). Dark CA activity or chemoautotrophic production was surprisingly high during the studied period, albeit one order of magnitude lower than the rates of photoautotrophic production. In the photic zone, these dark CA rates fluctuated between 0.20 and 145 mg C m⁻³ d⁻¹ (see Table 2) and maximum rates were observed at the subsurface (15–30 m depth). In the aphotic zone (the oxycline and bottom layer), dark CA fluctuated from 0.16 to 117 mg C m⁻³ d⁻¹. The highest values (up to 70 mg C m⁻³ d⁻¹) were located in the bottom layer near the sediments (see Fig. 4b). As with photosynthetic activity, chemolithoautotroph activity was always higher during upwelling-favourable periods (i.e., December 2007, January 2009).

Daily integrated rates for photoautotrophic production ranged between 0.14 and 7.63 mg C m⁻² d⁻¹, whereas daily

Table 1. Ammonium, nitrite, nitrate, nitrous oxide and methane content by layer (expressed as inventories) at Station 18 during April 2007–March 2009.

Time Series Cruise Cruise	Ammonium inventory mmol m ⁻²			Nitrite inventory mmol m ⁻²			Nitrate inventory mmol m ⁻²			Nitrous oxide inventory μmol m ⁻²			Methane inventory μmol m ⁻²		
	S-L	O-L	B-L	S-L	O-L	B-L	S-L	O-L	B-L	S-L	O-L	B-L	S-L	O-L	B-L
Apr-07	n-d	n-d	n-d	15.09	0.74	1.28	1295	709.8	904.7	834	611.6	805.6	122.8	828.1	998.3
May-07	15.05	6.37	6.75	8.68	0.96	0.78	106.5	534.4	761.5	517.1	610.3	820.4	599.8	480.3	1275
Jun-07	n-d	n-d	n-d	16.02	1.34	8.03	113.8	688.3	906.8	635.2	468.4	680.8	786.9	410.1	870.4
Jul-07	19.60	2.37	0.50	21.90	6.62	0.50	499.1	793.6	581.6	3892	929.2	951.1	189.9	241.0	142.6
Aug-07	13.02	6.13	2.49	11.36	12.48	2.80	605.8	613.5	487.1	628.3	748.4	924.1	697.3	821.0	1181
Sep-07	n-d	n-d	n-d	6.39	12.13	7.03	282.6	916.	629.9	321.0	846.9	788.1	364.9	824.1	651.9
Oct-07	n-d	n-d	n-d	2.60	3.07	1.83	237.1	1621.	847.3	226.5	1881	984.1	147.5	818.8	736.7
Dec-07	23.06	35.27	10.25	1.24	8.48	13.65	107.1	1586.	755.5	233.0	2464	1545	133.3	628.3	492.1
Jan-08	10.52	11.85	7.77	5.07	160.17	140.42	249.8	1309.	489.6	447.9	4400	2157	386.5	2486	1699
Feb-08	7.20	0.73	1.80	17.62	2.09	7.00	790.4	903.5	664.1	815.9	1131	1268	540.0	710.9	936.3
Mar-08	5.24	0.24	0.25	13.17	0.96	2.58	656.5	599.8	360.6	878.8	1043	1672	540.0	649.1	1226
Apr-08	35.55	0.98	0.65	11.33	6.78	8.58	740.9	896.7	682.5	755.7	1290	946.5	652.4	573.2	850.7
May-08	32.06	32.65	69.20	14.93	17.06	13.68	582.6	607.1	580.5	404.5	511.8	645.3	289.6	545.5	761.0
Jun-08	n-d	n-d	n-d	12.76	0.91	26.60	994.6	479.2	542.9	n-d	855.5	n-d	944.0	758.4	1439
Sep-08	8.55	0.98	12.15	6.08	0.56	4.22	738.6	525.9	660.2	1553	1309	1633	423.7	320.8	944
Oct-08	8.88	2.00	9.37	0.82	4.07	6.27	67.99	1195.9	627.7	404.8	1684	994.5	230.9	952.2	646.6
Nov-08	14.04	14.40	18.18	1.95	14.79	13.35	157.1	1380.3	608.1	653.8	3222	1578	115.2	585.2	824.2
Dec-08	4.49	101.12	98.61	14.71	108.04	132.34	444.9	828.6	333.8	2419	5885	1286	398.1	1153	1175
Jan-09	14.32	10.39	8.73	2.30	3.94	4.28	112.9	1267.3	668.9	269.1	1936	1405	143.8	699.8	905.5
Feb-09	2.84	11.83	9.10	9.15	9.60	21.41	312.4	1281.8	626.3	n-d	n-d	n-d	252.9	706.4	1030.5
Mar-09	9.53	4.95	11.38	7.11	4.95	18.9	417.5	1195	619.1	414.7	1067.8	816.3	111.3	1345	610
Average ^b	14.0	15.14	16.7	9.54	18.08	20.74	470.3	949.2	635.2	858.1	1644.8	1152.7	384.3	787.5	923.6

^a Gray colour indicates favourable upwelling period.; ^b average of values among months from April 2007 to March 2009 ($n = 19–24$).

S-L: comprised from surface to 1% irradiance. O-L comprised from <1% surface irradiance to 65 m depth. B-L comprised from 66 m depth to bottom; n-d: not determined.

integrated rates for chemoautotrophic production fluctuated from 8.06 to 2.85 mg C m⁻² d⁻¹. In the oxycline and bottom layers, daily integrated rates of dark CA reached 11.3 to 1.802 mg C m⁻² d⁻¹. On average, half of the chemoautotrophic production came from the photic layer (although values as high as 94% were observed in April 2008), whereas the other half of the dark CA was concentrated in the aphotic layer (see Table 2).

POC concentrations varied between 59.1 and 1.282 mg m⁻³ (Fig. 4c) and POC content decreased exponentially from the surface to the oxycline layer and then increased slightly towards the bottom. The POC concentration was remarkably high in the photic layer (see Fig. 4c). This distribution was a persistent feature during the study period and correlated well with the bacterioplankton distribution, which showed maximal abundance in surface and bottom waters (Galan et al., unpublished data). The C:N ratio of particulate organic matter was around 5.5 to 8 (data not shown) and increased with depth (i.e., the bottom water). $\delta^{13}\text{C}_{\text{POC}}$ was highly variable (-16.9 to -28.6%), although the water column was only 92 m in depth (see Fig. 4d). The vertical distribution of $\delta^{13}\text{C}_{\text{POC}}$ revealed an important vertical zonation that could reflect the influence of C metabolic processes and environmental conditions. In the photic layer, the mean value of $\delta^{13}\text{C}_{\text{POC}}$ was -19.7% and varied little ($\pm 2.2\%$ SD). In the oxycline, the mean

value of $\delta^{13}\text{C}_{\text{POC}}$ decreased to -22.2% and showed high monthly temporal variations ($\pm 2.8\%$ standard deviation), as reflected in the range of values: -17.7% to values as depleted as -28.6% (see Fig. 4d). These lighter $\delta^{13}\text{C}_{\text{POC}}$ values were accompanied by high NO_3^- , NO_2^- , and N_2O in summer (e.g., December 2007, January 2008). The average of $\delta^{13}\text{C}_{\text{POC}}$ in the bottom layer was 20.7%. The $\delta^{13}\text{C}_{\text{POC}}$ differed significantly among layers (t-student, $p < 0.05$) and this difference increased (t-student, $p < 0.01$) when the data were separated into non-upwelling and upwelling periods.

In order to look for relationships between dark CA and nutrients (that act as electron acceptors), several correlations were performed. At the oxycline, the N-oxide inventories (N_2O , NO_2^- , NO_3^-), but not NH_4^+ , showed significant high correlations with dark CA ($\rho = 0.57$, $p = 0.0008$; $\rho = 0.3$, $p = 0.028$; $\rho = 0.5$, $p = 0.002$, respectively). These significant correlations between N-species inventories and dark CA rates indicated that AAO and ANO could be responsible for a fraction of dark CA, producing NO_2^- and NO_3^- , respectively. In the bottom layer, NH_4^+ showed a stronger correlation with dark CA rates compared to the N-oxides (except NO_3^-) ($\rho = 0.39$, $p = 0.02$). In the surface layer, photo CA rates are subjected to rapid nutrient and C turnover is driven largely by light energy. The CH_4 inventory was inversely correlated with dark CA within the oxycline ($\rho = -0.58$, $p = 0.02$).

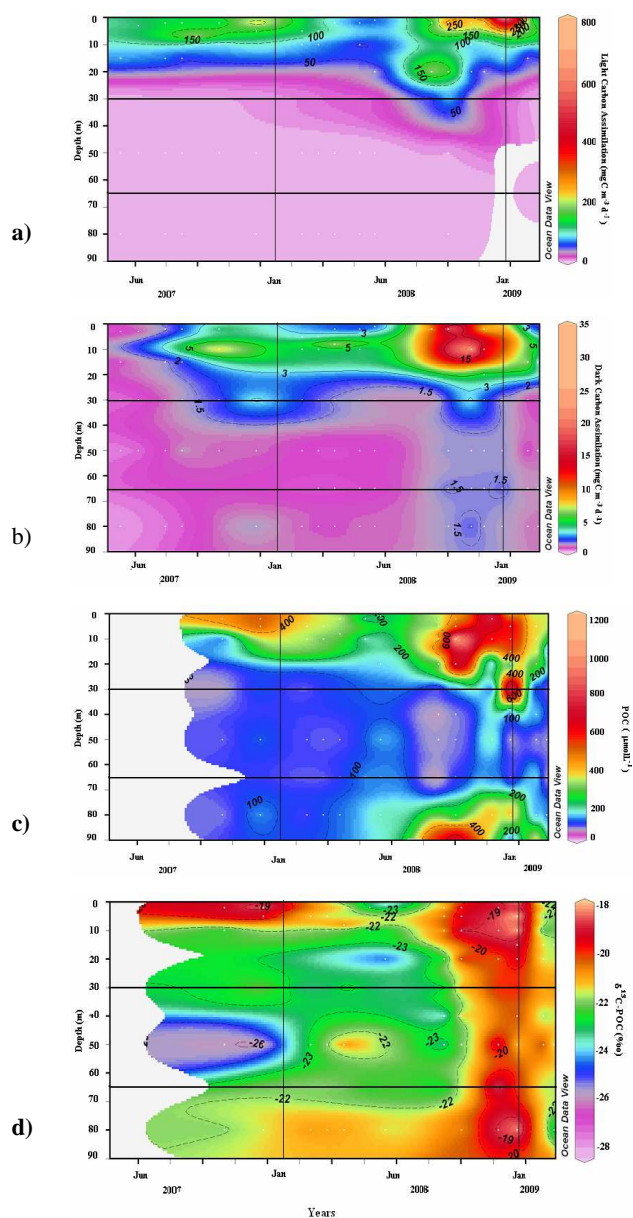


Fig. 4. Seasonal variation in autotrophic carbon fixation: (a) photoautotrophic carbon assimilation, (b) dark carbon assimilation, (c) natural C isotopic composition of POM, and (d) POC concentration (data from April 2007 to March 2009).

3.4 Dark carbon assimilation and N₂O and CH₄ cycling associated with AAO and AMO

Figure 5 shows a representative time course for the accumulation of ¹³C in POC, N₂O and CH₄ production and consumption during incubation experiments performed at Station 18, using a control (without any addition) and ATU and GC7 inhibitor experiments. ATU should inhibit NH₄⁺ and CH₄ oxidation and, therefore, may decrease dark CA, N₂O production, and CH₄ consumption due to the inhibition

of their monooxygenase systems. In contrast, GC7 acts on archaeal nitrifying and methanotrophs and, therefore, on their metabolic pathways associated with CA and N₂O and CH₄ cycling.

Table 3 shows the results of experiments carried out in the oxycline and the bottom layer along with other environmental conditions measured at these sampling times. Dark ¹³CA rates in the control experiment (without any inhibitor) ranged from 0.21 to 4.91 mg C m⁻³ d⁻¹, peaking in January 2009 (MI-LOCO cruise, see Table 3 and Fig. 5). These rates were of the same order of magnitude as the net rates obtained during the monthly in situ incubations (see Fig. 4b). With the addition of ATU, dark CA was effectively reduced by 28 to 48% with respect to the control experiment (estimated by average rates; see Table 3, Fig. 5). The effect of GC7 on archaeal CA rates was more evident in bottom waters, where a 76% decrease was observed. Overall, dark CA rates were higher in samples amended with the ATU inhibitor compared to GC7 (on average, 25 and 51% higher at 30 and 80 m depth, respectively; see Table 3).

In the gas cycling experiments (net cycling), N₂O accumulated in both layers. This means that N₂O was accumulated at net rates of 8.88 to 42.9 nM d⁻¹, the highest rates being observed in upwelling periods in both the oxycline (40 nM d⁻¹) and bottom (43 nM d⁻¹) layer. ATU usually had a significant effect on gas cycling, reducing N₂O accumulation (see Table 3); GC7 also reduced the net N₂O rates. In contrast, CH₄ was consumed in both layers at rates fluctuating between 0.41 and 26.8 nM d⁻¹. This suggests that the processes responsible for CH₄ consumption were higher than the processes producing it. ATU and GC7 also affected net gas cycling, most of the time producing three and ten-fold increases in its consumption rate (see Table 3).

4 Discussion

The continental shelf water, off the coast of central Chile, is one of the most productive marine ecosystems in the world, sustaining the highest primary and fisheries productivity in the global ocean. This high productivity is usually explained by the coastal upwelling of subsurface, nutrient-rich waters to the surface. This process is driven by the winds and fertilizes the surface waters, promoting phytoplankton blooms and the transfer of organic matter and energy to higher trophic levels and towards the surface sediments (Escribano et al., 2004; Farías et al., 2004). The magnitude and observed temporal variability of biological productivity in this system, however, cannot be solely explained by the effect of physical factors related to the onset of the upwelling process and subsequent phytoplankton C and N uptake. The presence of a persistent redoxcline and oxygen-deficient waters below the euphotic zone during active and non-active upwelling periods might also favour chemoautotrophic carbon assimilation in dark conditions.

Table 2. Light and dark carbon assimilation (volumetric range and depth integrated values) and natural C isotopic ratio for photic layer and aphotic layer (including oxycline and bottom layer) at Station 18 during April 2007–March 2009.

Time serie cruises	Photic Layer Depth m	Photo $\rho^{13}\text{C}$ range $\text{mg m}^{-3} \text{d}^{-1}$	Dark $\rho^{13}\text{C}$ range $\text{mg m}^{-3} \text{d}^{-1}$	Photic Layer			Dark $\rho^{13}\text{C}$ range $\text{mg m}^{-3} \text{d}^{-1}$	Aphotic Layer			Total water column ^a Dark $\sum \rho^{13}\text{C}$ $\text{mg m}^{-2} \text{d}^{-1}$
				Photo $\sum \rho^{13}\text{C}$ $\text{mg m}^{-2} \text{d}^{-1}$	Chemo $\sum \rho^{13}\text{C}$ $\text{mg m}^{-2} \text{d}^{-1}$	$\delta^{13}\text{C}_{\text{Corg}}^{\text{b}}$ ‰		Dark $\sum \rho^{13}\text{C}$ $\text{mg m}^{-2} \text{d}^{-1}$	$\delta^{13}\text{C}_{\text{Corg}}^{\text{c}}$ O-L ‰	$\delta^{13}\text{C}_{\text{Corg}}^{\text{d}}$ B-L ‰	
Apr-07	45	69.9–96.4	0.30–0.46	2521	10.95	n-d	0.24–0.38	15.5	n-d	n-d	26.4
May-07	40	44.8–125	0.28–0.39	2514	9.69	n-d	0.20–0.24	13.0	n-d	n-d	22.7
Jun-07	45	66.3–91.3	0.20–0.25	2402	11.20	v-d	–	–	n-d	n-d	–
Jul-07	31	56.3–144	0.24–0.32	2901	8.06	n-d	0.16–0.32	11.3	n-d	n-d	19.4
Aug-07	36	1.83–123	1.43–2.14	1203	53.77	n-d	0.53–2.35	87.6	n-d	n-d	14.1
Sep-07	23	0.65–366	n-d	3411	n-d	n-d	n-d	n-d	n-d	n-d	–
Oct-07	10	19.2–25.9	6.25–12.5	232	87.54	–21.55	0.45–0.62	142	–24.63	–22.28	230
Dec-07	10	149–404	70.2–84.9	4428	1149	–17.21	1.17–6.23	807	–24.86	–21.96	19.6
Jan-07	14	n-d	n-d	n-d	n-d	–17.82	n-d	–	–19.82	–19.51	–
Feb-08	34	0.42–173	0.92–3.27	2093	78.94	–22.29	0.63–0.99	58.6	–24.02	–20.88	13.8
Mar-08	41	2.75–80.9	0.90–2.33	1290	53.39	–22.65	0.40–0.50	26.4	–23.07	–21.62	79.8
Apr-08	32	0.16–75.6	0.28–15.7	1748	235.7	–18.98	0.38–0.74	16.0	–19.67	–21.29	26.4
May-08	33	0.75–13.5	0.38–1.55	135	23.18	–24.96	0.54–1.51	51.4	n-d	n-d	49.62
Jun-08	47	0.58–42.1	0.42–0.87	549	19.56	–25.48	0.49–0.66	27.3	n-d	n-d	46.8
Sep-08	44	1.61–274	0.22–1.31	4295	21.08	–22.38	n-d	–	–25.02	–23.86	2.62
Oct-08	16	224–435	29.9–44.0	6805	725.8	n-d	1.24–101	1802	n-d	n-d	25.27
Nov-08	15	46.7–200	32.5–38.4	1387	109.1	–17.64	1.22–70.0	991	–20.36	–20.83	13.51
Dec-08	26	2.81–134	1.23–4.92	1590	109.1	–1974	1.16–1.46	67.0	–19.11	–18.36	18.5
Jan-09	12	0.75–825	0.66–145	7626	2851	–17.94	1.24–1.86	71.7	–20.64	–19.5	29.24
Feb-09	18	0.43–155	0.52–8.29	1995	191	–21.59	0.37–0.99	32.0	–21.11	–21.47	22.3
Mar-09	19	0.41–84.2	0.64–1.56	1282	37.1	–22.03	0.90–1.35	52.8	–21.17	–23.43	90.9

^a Total dark CA in the whole water column (integration from surface to 92 m depth).

^b Average $\delta^{13}\text{C}_{\text{Corg}}$ for S-L ($n = 2–4$) per time series cruise.

^c Average $\delta^{13}\text{C}_{\text{Corg}}$ for the O-L ($n = 2–3$) per time series cruise.

^d Average $\delta^{13}\text{C}_{\text{Corg}}$ for the B-layer ($n = 2–3$) per time series cruise.

n-d: not determined.

Table 3. Rates of dark carbon assimilation ($\text{mg C m}^{-3} \text{d}^{-1}$) and N_2O and CH_4 cycling (nM d^{-1}) along with environmental conditions at the oxycline and bottom layer.

Cruises Layer depth	NICCHEX I		NICCHEX II		MI-LOCO I	
	O-L 30 m	B-L 80 m	O-L 30 m	B-L 80 m	O-L 30 m	B-L 80 m
Date	Jan 2008	Jan 2008	Sep 2008	Sep 2008	Jan 2009	Jan 2009
Environmental Variables						
Temperature ($^{\circ}\text{C}$)	10.5	10.2	11.4	10.3	10.5	10.5
O_2 (mL L^{-1})	6.24	3.12	149	13.4	72.7	1.78
NH_4 (μM)	0.12	1.04	0.04	0.10	0.31	0.40
N_2O (nM)	62.1	49.6	23.5	40.3	31.4	19.6
CH_4 (nM)	41.5	132.7	9.44	40.6	9.14	37.1
Dark CA ($\text{mg C m}^{-3} \text{d}^{-1}$)						
Dark CA rate	n-d	3.53±1.40	0.24±0.04	0.21±0.04	0.49±1.13	4.91±0.77
Dark CA + ATU rate	n-d	2.54±0.21	n-d	0.18±0.05	0.44±0.03	2.54±0.17
Dark CA + GC7 rate	n-d	0.47±0.1	n-d	0.16±0.06	0.36±0.04	1.31±0.41
% of Dark CA rate sensitive to ATU	n-d	27.9	–	14.3	10.2	48.0
% of Dark CA rate sensitive to GC7	n-d	76.3	–	24.8	26.5	73.3
Gas Cycling (nM d^{-1})						
^a Net N_2O	40.05±3.55 32.37±1.51	23.36±0.58 22.01±1.57	8.88±2.88	16.80±6.00	22.41±2.93	42.96±8.76
N_2O + ATU	30.05±5.35		5.21±.85	13.27±1.56	13.81±3.84	7.22±2.90
N_2O + GC7	25.32±5.24	11.42±3.37	n-d	n-d	n-d	n-d
^a Net CH_4	–1.60±0.55 –3.00±1.20	–0.41±0.07 –1.32±0.82	–1.68±0.72	n-d	–5.30±2.88	–26.83±8.16
CH_4 + ATU	–7.68±0.96	–0.87±0.07	–1.78±0.41	n-d	–18.00±2.4	–23.76±6.24
CH_4 + GC7	n-d	–13.26±0.50	n-d	n-d	n-d	–91.20±7.44

^a Values are given for two independent experiments.

n-d: not determined.

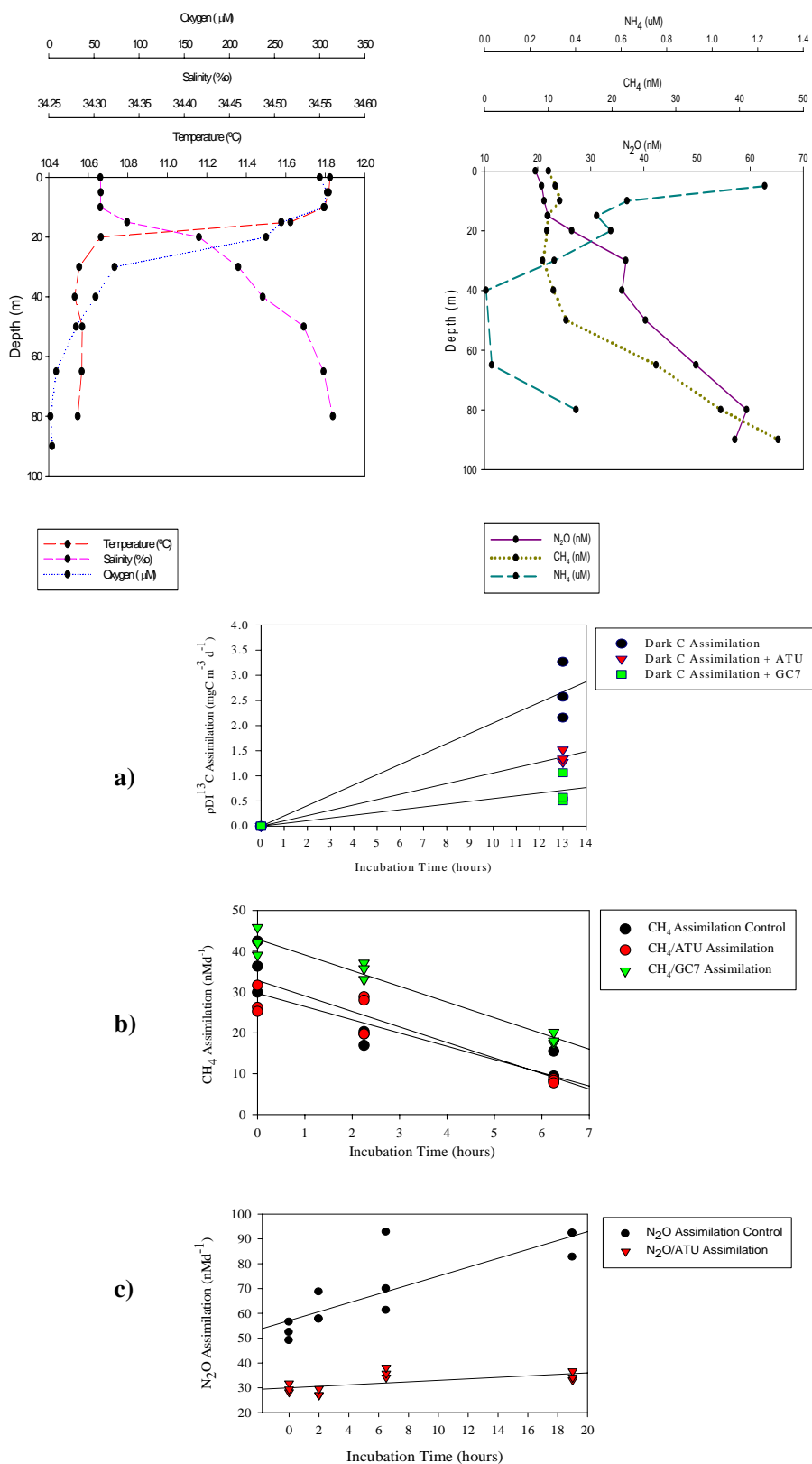


Fig. 5. Profiles of hydrographic and oceanographic conditions in the water column at the time of the experiment (MI-LOCO cruise, January 2009) Below time course experiments showing different treatments (control, ATU and GC7-amended incubations): (a) dark carbon assimilation, (b) CH₄ (with linear regression), and (c) N₂O (with linear regression).

Dark CA, which has been also observed at high rates in some redoxclines (e.g., Zopfi et al., 2001), was explored during this study as a possible explanation for such variability.

Oxygen is undoubtedly a chemical forcing factor in this coastal upwelling ecosystem because of the tight link between its vertical distribution and its consumption due to the respiration of sinking POC. Respiration is also enhanced by upwelling events in austral spring-summer, when more electron donors (organic matter) are available to be respired by microorganisms. The vertical distribution of nutrients and gases also reflects the seasonality of C cycling, which, in turn, strongly affects the microbial ecology and geochemistry of most coastal ecosystems.

It is known that all reduced species can act as electron donors for dark CA or chemolithoautotrophic processes. In order to determine how much chemical energy is cycling in this system, the size of pools for reduced species was estimated assuming that NH_4^+ , NO_2^- , and CH_4 are being oxidized in the study area with O_2 as the electron acceptor. Electron donor inventories for each layer were estimated by linear depth interpolations for each predefined layer. These inventories (see Table 2) were then converted into chemical energy, taking into account Gibbs free energy ($-\Delta G^\circ$). This means the enthalpy of a reaction (ΔH) of different electron donors with O_2 as an electron acceptor, assuming that these electron donors are completely oxidized by O_2 in the water column. The ΔG° from AAO, ANO, and AMO are -274.7 , -74.1 , and -890 kJ mol^{-1} , respectively (Madigan, 2003). The sum of these reactions is -335.7 kJ m^{-2} for the study period (April 2007–March 2009), which is a large amount of chemical energy in terms of kJoules per mol of oxidized species. Most of the chemical energy (about 70%) comes from NH_4^+ oxidation during upwelling favourable periods, although the oxidation of Fe and S species (not considered in this estimation) could also be important in the area.

4.1 What is the relative importance of chemo- vs. photoautotrophic production?

Chemolithoautotrophy is the non-photosynthetic biological conversion of C1 molecules (usually CO_2 or CH_4) into organic matter. Table 2 shows the integrated photo vs. chemoautolithotrophic production in the whole water column. Integrated rates of chemoautotrophic CA were as high as $2.924 \text{ mg C m}^{-2} \text{ d}^{-1}$ and they represented between 0.7 (July 2007) and 50% (October 2007 and 2008) of the integrated photoautotrophic production (up to $7.626 \text{ mg C m}^{-2} \text{ d}^{-1}$). An average value of 20.3% was estimated for the two-year period of monthly sampling. Dark CA rates in the photic layer reached between 0.3 and 27% of the total autotrophic production, whereas dark CA rates in the aphotic layer (or the oxycline plus bottom layer) represented between 0.4 and 40% (see Table 3). Figure 6 shows total integrated chemolithoautotrophic and photoautotrophic rates per layer (both photic and aphotic)

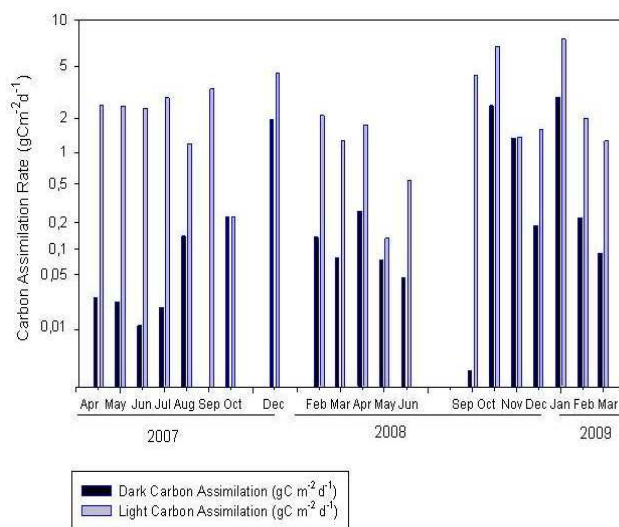


Fig. 6. Total integrated chemolithoautotrophic and photoautotrophic rates along time sampling; the Y-axis is on a logarithmic scale.

and date of sampling. These values suggest the existence of a large pool of organic matter of chemolithoautotrophic origins in both layers (photic and aphotic) that has not been accounted for in this or any other coastal upwelling ecosystem.

In the surface layer, dark CA is surprising high and can be ascribed to chemolithoautotrophic production co-existing with photoautotrophic production that also provides inorganic elements to fuel this chemoautotrophic activity. In fact, notorious NH_4^+ recycling through bacterioplankton communities and flagellates has been found in the surface waters of central Chile (Böttjer and Morales, 2007; Vargas et al., 2007). Part of this recycling can be channeled through nitrification, providing regenerated NO_3^- and organic matter by chemoautotrophy, which, in turn, sustains microbial food webs. However, given the complex interactions and metabolisms associated with this microbial web, a fraction of this dark CA could be sustained by anaerobic CO_2 fixation via oxaloacetate and pyruvate production (Sorokin, 1993), which is the most plausible physiological pathway that could be found in this kind of ecosystem. However, the relative importance of these reactions and their capacity to support dark carbon assimilation cannot be discerned with the bulk ^{13}C methodology.

Other evidence of high rates of ammonium uptake by phytoplanktonic and bacterioplanktonic communities is also observed in similar upwelling ecosystems (Lipschultz et al., 1990; Fernandez et al., 2009), indicating that ammonium is quickly recycled in these ecosystems and that an important fraction of primary production is sustained by regeneration. These results combine well with our observations and could

indicate that the chemolithotrophic AAO community is sustaining its energetic demand by oxidizing N-compounds although the rate of ammonium oxidation is sometimes not as rapid as the rate at which it is being produced (intense NH_4^+ regeneration), thereby allowing occasional NH_4^+ accumulations in the photic layer (Fig. 3c).

In deeper redox systems, away from the reach and influence of light (e.g., the Black Sea, Cariaco Basin, and Baltic Sea), dark CA rates of up to 2.1, 30, and 18 $\text{mg C m}^{-3} \text{d}^{-1}$ have been reported (Taylor et al., 2001; Pimenov and Neretin, 2006; Jost et al., 2008). In the Black Sea, integrated chemolithoautotroph rates in the range of 300 to 800 $\text{mg C m}^{-2} \text{d}^{-1}$ were measured and accounted for 50 to 80% of the primary production, whereas in the Cariaco Basin, dark CA represented on average 70% of the primary production. Likewise, in the Mariager Fjord, dark CA accounted for 37% of total C fixation, but rates were as high as 1.092 $\text{mg C m}^{-3} \text{d}^{-1}$, leading to the possibility of an important heterotrophic CA activity within a narrow chemocline (Zopfi et al., 2001). Our rates fall in the highest range of these measurements (for comparison, see Table 4). Nevertheless, it is important to note that those systems are euxinic environments in which chemolithoautotrophy is fuelled by reduced S-species. In contrast, the upwelling area off central Chile does not seem to involve sulphide utilization (HS^- levels are within nanomolar values) but exhibit large NH_4^+ levels, often on the μmolar scale. In addition, sediments underlying the upwelling area off central Chile have low pore water HS^- concentrations ($<2 \mu\text{M}$) but high SO_4^{2-} reduction rates (Thamdrup and Canfield, 1996). The massive occurrence of mat-forming *Thioploca*, which can oxidize sulphide by reducing their internally stored nitrate, explains part of the low observed HS^- levels in the study area (Jorgensen and Gallardo, 1999). In this sense, the absence of HS^- in this system, which can act as a powerful inhibitor of nitrification at high concentrations (Joyce and Hollibaugh, 1995), could explain the measured chemolithoautotrophic dark CA rates that are likely to be later channeled towards nitrifying microbes. The strong correlations found between N oxidized species inventories and dark CA rates, but not with NH_4 , also confirm that nitrification is consuming NH_4^+ and producing N_2O , NO_2^- , and NO_3^- (see Fig. 4a, b).

Moreover, our results revealed a significant vertical variation of $\delta^{13}\text{POC}$ in spite of continuous water column mixing due to vertical advection (summer time) or turbulent mixing (winter time). Although the isotopic signal of sinking photosynthetic organic matter should reflect its origin, the sinking organic matter associated with the oxycline had a different isotopic C signal (reaching values as light as -28.6‰) compared to those observed in the photic layer (reaching values as heavy as -16.9‰). The distinct isotopic composition of the oxycline was possibly associated with chemolithoautotrophic organisms

whose presence generally resulted in greater use of the lighter isotope and, as a result, a more negative isotopic composition of the chemosynthetically produced C compared to that C of photosynthetic origin (Fry et al., 1991; Hayes, 2001). According to the above, the observed vertical pattern (see Fig. 4d) confirms the occurrence of chemolithoautotrophic production leading to predominantly organic matter produced in situ. A similar pattern was found by Coban-Yildiz et al. (2006) in the Black Sea. A plot of C: N vs. $\delta^{13}\text{C}_{\text{org}}$ -POM lead us to exclude the possibility of terrestrial influence, despite the proximity of our station to the coast (18 nm) and its location over the continental shelf, receiving high fresh water discharges from the Bio Bio River, mostly in wintertime.

4.2 Are nitrifying and methanotrophic activities responsible for dark C assimilation?

The ATU compound used in this study inhibits the ammonium monooxygenase enzyme (AMO); however, it could also affect methane monooxygenase enzyme activity. Therefore, these communities could potentially be included in our carbon fixation experiments. On the contrary, it is improbable that ATU exerts an influence on the anammox process, as recently proven by Jensen et al. (2007). However, ATU could potentially influence the activity of the AMO enzyme of ammonium-oxidizing archaea (AOA). Thus, the 30% reduction of dark fixation rates in the ATU treatment with respect to the control is the most direct evidence that this dark CA is associated with AAO (both bacteria and archaea) and maybe AMO. Most of the total dark-carbon fixation ranged between 0.16 and 1.5 $\mu\text{g C L}^{-1} \text{d}^{-1}$ (Table 2); thus, if 30% of this rate was sensitive to ATU, a carbon fixation to NH_4^+ oxidation molar ratio (C/N) of ~ 8 (Bianchi et al., 1997) results in NH_4^+ oxidation values of ~ 0.24 to 0.88 $\mu\text{mol L}^{-1} \text{d}^{-1}$. This range of values is very reasonable for the study area and is supported by estimations of the turnover time of the ammonium pool and rates of ammonium oxidation measured in the study area by chemical assays (Molina et al., unpublished data) and isotopic techniques (Fernandez et al., unpublished data).

The GC7 inhibitor used in this study is known to affect archaeal protein synthesis (Jansson et al., 2000) and has been used in the past to explore the significance of methanogenic archaea at the time-series Station 18 (Levipan et al., 2007). The reduction by 70% of dark CA in GC7 experiments confirms the presence of archaea and proves them capable of CA in the dark at the oxycline and near-bottom depth level. Using inhibitors, we obtained rates for ATU-sensitive microbes (e.g., AAO and AMO bacteria) that were around half the values associated with the archaeal groups (1.27 vs. 0.6 $\text{mg C m}^{-3} \text{d}^{-1}$) (see Table 3). This experimental approach suggests the occurrence of archaeal and bacterial chemolithoautotrophic microbes in the same experimental samples.

Table 4. Literature and present estimates of Dark Carbon assimilation rates in the main redoxclines of the ocean.

Area	Dark CA rates mg C m ⁻³ d ⁻¹	Cell abundance Cell mL ⁻¹	Method	Source
^a The Black sea	0.45–2.10 (0.11–0.20) 0.30–0.8	1.5–5.5 × 10 ^{5e}	¹⁴ C	Pimelov and Neretin 2006 Sorokin <i>vide</i> Pimelov and Neretin 2006
^b The Baltic sea	2.40–18.0 8.4–16.8	1.16–1.65 × 10 ^{6f}	¹⁴ C ¹⁴ C <i>in vitro</i>	Jost et al., 2008 Labrenz et al., 2005
^c Cariaco Basin	5–30 (0.32–1.90) 2.4–31.2	1.9–7.4 × 10 ^{5e}	¹⁴ C	Taylor et al., 2001 Ho et al., 2004
^d Mariager Fjord	115.5–1092 (0.12)	n-d		Zopfi et al., 2001
Central Chile shelf water	0.16–70 (0.02–2.92)	5 × 10 ⁵ –4 × 10 ^{6f}	¹³ C	This study

Values in parenthesis are integrated rates (g m⁻² d⁻¹).

^a The Black Sea; rates measured at redoxcline (100–300 m depth) in absence of O₂ and high levels of HS⁻.

^b Gotland Deep and Landsort deep redoxcline located at 120–150 m.

^c Cariaco Basin 10° 50' N; 64° 66' W; redoxcline at 240–450 m depth HS⁻ accumulation up to 75 μmol L⁻¹.

^d Mariager Fjord (Denmark) 56° 39' N; 09° 58' E. 25 m depth; rates measured at redoxcline (13–15 m). HS⁻ as high as 75 μmol L⁻¹ was measured.

^e DAPI counting.

^f flow cytometry counting.

n-d: not determined.

Total bacterial abundances (measured by flow cytometry) can reach 4 × 10⁶ cell mL⁻¹ in surface waters and 1 × 10⁶ cell mL⁻¹ in near-bottom waters during upwelling-favourable periods (Alarcón and Ulloa, unpublished data). Archaea also represent a significant fraction of the total prokaryotic community off central Chile, accounting for about 50% abundance at the bottom and up to 25% in the surface waters of our study area (Levipan et al., 2007; Quiñones et al., 2009). Based on DAPI counting, the abundance of archaea has been estimated to be close to 5 × 10⁵ cells mL⁻¹ in the bottom water and crenarchaeota can potentially reach 30% of the total prokaryotic community (Belmar, personal communication, 2009).

Taking into account the reported abundance of each group at 80 m depth, we estimated a CA rate of around 63 fg cell⁻¹ d⁻¹ for archaea and around 60 fg cell⁻¹ d⁻¹ for bacteria. The average C content of prokaryotic microorganisms previously reported in the study area was ~43 fg cell⁻¹ (Levipan et al., 2007a), indicating the capacity of chemolithoautotrophic production to meet the daily C demand of chemoautotrophic C fixers, at least during the spring-summer period. Additionally, the calculated specific rates of dark CA ranged from 0.005 up to 0.05 h⁻¹, reflecting the existence of an active, relatively rapidly growing chemoautotrophic community whose components have yet to be determined.

Although we cannot evaluate the importance of a specific pathway (AAO and AMO), the availability of substrates such as NH₄⁺ and CH₄ in the water column suggest that

most of this dark CA occurs by their oxidation. Specific rates (h⁻¹) in both cases changed with the addition of ATU or GC7 (as compared to total dark CA). When excluding ATU-sensitive NH₄⁺ and CH₄ oxidizers, the specific CA rates were lower than the specific CA obtained when excluding archaeal microbes. This suggests that the chemolithoautotrophic C utilization per unit of POC per time is sensitive to the community structure and archaeal C fixers are important players in the C turnover of the system. We can, therefore, expect a variable but important proportion of active prokaryotes to co-exist year-round with an equally variable photoautotrophic community.

Until now, very little effort has been made to distinguish dark CA from different groups of microbes. Some advances were performed in the Black Sea and Cariaco Basin, where most of the microbes were bacteria associated with the S-cycle and concentrated at the redoxcline (Pimenov and Neretin, 2006; Li et al., 2008). Off the Namibian coast (~23° S), chemolithotrophic bacteria affiliated with γ-proteobacteria and accounting for approximately 20% of the bacterioplankton in sulphidic waters can create a buffer zone between the toxic sulphidic subsurface waters and the oxic surface waters (Lavik et al., 2009).

4.3 N₂O and CH₄ cycling in the water column

Net N₂O cycling rates were positive, indicating that N₂O is being produced in the water column (see Table 3). Four main pathways have been described as leading to N₂O production

(Fariás et al., 2009): 1) partial denitrification, or NO_2^- reduction to N_2O ; 2) nitrite-ammonification, the conversion of NO_3^- to NH_4^+ ; 3) nitrification, including NH_4^+ oxidation to NO_2^- ; and 4) nitrifier denitrification. But so far, only one process – total denitrification – is known to consume N_2O by reducing it to N_2 under extremely low O_2 ($<4.4 \mu\text{M}$) or suboxic conditions (Elkins et al., 1978; Farías et al., 2009). Thus, the amount of N_2O in the ocean depends on a balance of N_2O production and consumption processes. The prevalence of N_2O accumulation in all the experiments indicates that production processes are predominant. The reduction of N_2O cycling rates in experiments treated with ATU (see Table 3) suggests that NH_4^+ oxidation is one of these N_2O producing processes in the study area. The reduction of net N_2O accumulation by ATU indicates that N_2O is also being produced by partial denitrification (NO_2^- reduction to N_2O), but its total reduction to N_2 is not ruled out in the bottom layer. Although NH_4^+ oxidation and CA rates are coherent with reported NH_4^+ oxidizing activities, there are no further elements to allow an assessment of the potential contribution of other NH_4^+ oxidizers or even other potentially ATU-sensitive communities (e.g., aerobic methanotrophs). However, N_2O cycling and dark CA rates were also reduced in GC7-amended experiments, providing direct evidence that NH_4^+ oxidizing archaea are present and active in the study area.

Net CH_4 cycling rates were negative in both the oxycline and bottom layers, indicating that CH_4 is being consumed (see Table 3). Interestingly, CH_4 consumption in the bottom layer was lower (see Table 3), suggesting that methanogenesis could be also acting in the same layer. However, the lack of an adequate sampling resolution in the water column and the difficulty of measuring processes and gas cycling rates near the sediments preclude determining the source of the observed CH_4 . Among methanotrophic or methane-consuming microbes, the anaerobic methane-oxidizer archaea in consortium with sulphate-reducing bacteria can remove a large fraction of CH_4 (Schubert et al., 2006). However, given the predominance of hypoxic conditions, the high affinity of methane mono-oxygenase enzyme for O_2 ($0.1\text{--}16 \mu\text{mol L}^{-1}$; Trotsenko and Murrell, 2008) and the response of net CH_4 cycling rates to ATU inhibition, AMO is the most likely process using CH_4 off central Chile.

5 Conclusion and perspectives

Our study reveals that integrated dark CA fixation within the redoxcline and the aphotic zone of the coastal area off central Chile represents, on average, 20% of total autotrophic production. This fraction is sustained by a large amount of chemical energy that comes mainly from ammonium and less from nitrite and methane. Increased chemoautotrophic activity as a response to upwelling-favourable periods is

due to the high biological production observed. Aerobic ammonium oxidation is one of the main chemolithotrophic processes (up to 48% of total chemosynthesis) occurring in the study area. From an ecological point of view, the existence of chemolithotrophic processes that can channel all these chemical energies make this upwelling ecosystem more efficient in terms of organic matter cycling than other eutrophic systems.

From a global point of view, these results have important environmental implications because of the leading role of O_2 in controlling organic matter dynamics through heterotrophic or autotrophic processes. Hypoxia is a well-known feature of major eastern boundary currents where coastal upwelling occurs (Helly and Levin, 2004). The development of severe hypoxia has been reported by Naqvi et al. (2000) in the Arabian Sea and by Grantham et al. (2004) in the northeast Pacific. Although the mechanisms for these events are different – one is explained by increased eutrophication and the other by changes in oceanic currents – both are being influenced by global climate change (Deutsch et al., 2008; Stramma et al., 2008). An expected consequence of climate change is the expansion of O_2 -deficient waters, because of the decrease in O_2 -solubility due to the warming of the ocean's surface layer. Higher temperatures also imply greater thermal stress, which could lead to stronger winds and, therefore, persistent upwelling (Bakun, 1990). The possible responses of coastal upwelling ecosystems include changes in the microbial community structure and diversity as well as strong biogeochemical transformations in the main known biogeochemical processes (e.g., nitrification and photosynthesis) currently driving atmospheric-oceanic exchanges of carbon and nitrogen (as CO_2 and N_2O). Consequently, if hypoxic conditions intensify in the world ocean, the increased importance of chemical energy should be translated into a highly active chemolithoautotrophic community.

Acknowledgements. This research was funded by the FONDECYT Grant #1070518 and partially by the Gordon and Betty Moore Foundation (MI-LOCO I cruise). We thank the captain and crew of the Kay Kay research vessel and colleagues who facilitated our observations and sample collection, as well as Mauricio Gallegos and Jamey Redding for assisting with the IRMS and field analyses, respectively. Once again, we are thankful to Antony Davies for improving the English of the text and Osvaldo Ulloa for critical reviews of this manuscript.

Edited by: J. Middelburg

References

- Bakun, A.: Global climate changes and the intensification of coastal upwelling. *Science*, 241, 148–201, 1990.
- Bange, H., Rapsomanikis, S., and Andreae, M. O.: Nitrous oxide in coastal waters, *Global Biogeochem. Cy.*, 10, 197–207, 1996.

- Coban-Yildiz, Y., Altabet, M. A., Yilmaz, A., and Suleyman, S.: Carbon and nitrogen isotopic ratios of suspended particulate organic matter (SPOM) in the Black Sea water columns, *Deep Sea Res. II.*, 53, 1875–1892, 2006.
- Cornejo, M., Farías, L., and Gallegos, M.: Seasonal variability in N_2O levels and air-sea N_2O fluxes over the continental shelf waters off central Chile ($\sim 36^\circ S$), *Prog. Oceanogr.*, 75, 383–395, 2007.
- Crutzen, P. J.: Methane's sink and source, *Nature*, 350, 380–391, 1991.
- Daneri, G., Dellarossa, V., Quiñones, R. A., Jacob, B., Montero, P., and Ulloa, O.: Primary production and community respiration in the Humboldt Current System off Chile and associated oceanic areas, *Mar. Ecol. Prog. Ser.*, 197, 41–49, 2000.
- Deutsch, C., Emerson, S. R., and Thompson, L.: Fingerprints of climate change in North Pacific oxygen, *Geophys. Res. Lett.*, 32, L16604, doi:10.1029/2005GL023190, 2005.
- Elkins, J. W., Wofsy, S. C., Mcelroy, M. B., Kolb, C., and Kaplan, W. A.: Aquatic sources and sinks for nitrous oxide, *Nature*, 275, 602–606, 1978.
- Eppley, R. W.: New production: history, methods, problems, in: *Productivity of the ocean: present and past*, edited by: Berger W. H., Smetacek, V. S., and Wefer, G., John Wiley & Sons Limited, Chichester, New York, 85–97, 1989.
- Escribano, R., Daneri, G., Farías, L., Gallardo, V. A., González, H. E., Gutierrez, D., Lange, C. B., Morales, C. E., Pizarro, O., Ulloa, O., and Braun, M.: Biological and chemical consequences of the 1997–1998 El Niño in the Chilean coastal upwelling system: a synthesis, *Deep Sea Res.*, 51, 2389–2411, 2004.
- Farías, L., Graco, M., and Ulloa, O.: Nitrogen cycling in continental shelf sediments of the upwelling ecosystem off central Chile, *Deep Sea Res. II.*, 51, 2491–2505, 2004.
- Farías, L. and Cornejo, M.: Effect of seasonal change in bottom water oxygenation on sediment N-oxide and N_2O cycling in the coastal upwelling regime off central Chile ($36.5^\circ S$), *Prog. Oceanogr.*, 75, 561–575, 2007.
- Farías, L., Castro-González, M., Cornejo, M., Charpentier, J., Faúndez, J., Boontanon, N., and Yoshida, N.: Denitrification and nitrous oxide cycling within the upper oxycline of the oxygen minimum zone off the eastern tropical South Pacific, *Limnol. Oceanogr.*, 54, 132–144, 2009.
- Fry, B., Jannasch, H. W., Molyneaux, S. J., Wirsén, C. O., Muramoto, J. A., and King, S.: Stable isotope studies of the carbon, nitrogen and sulfur cycles in the Black Sea and Cariaco trench, *Deep-Sea Res.*, 38, S1003–S1019, 1991.
- Ginestet, P., Audic, J., Urbain, V., and Block, J.: Estimation of nitrifying bacterial activities by measuring oxygen uptake in the presence of the metabolic inhibitors Allylthiourea and Azide, *Appl. Environ. Microb.*, 64, 2266–2268, 1998.
- Grantham, B. A., Chan, F., Nielsen, K., David, S., Fox, D. S., Barth, J. A., Huyer, A., Lubchenco, J., and Menge, B. A.: Upwelling-driven nearshore hypoxia signals ecosystem and oceanographic changes in the northern Pacific, *Nature*, 429, 749–754, 2004.
- Grasshoff, K., Ehrhardt, M., and Kremling, K.: *Methods of seawater analysis: Second Edition*. Springer-Verlag, Basel, Switzerland, 419 pp., 1983.
- Hanson R. and Hanson, T. E.: Methanotrophic Bacteria, *Microb. Rev.*, 60, 439–471, 2000.
- Hayes, J. M.: Fractionation of carbon and hydrogen isotopes in biosynthetic processes, in: *Stable isotope geochemistry*, edited by: Valley J. W. and Cole, D. R., *Rev. Mineral Geochem.*, 43, 225–278, 2001.
- Helly, J. and Levin, L.: Global distribution of naturally occurring marine hypoxia on continental margins, *Deep-Sea Res.*, 51, 1159–1168, 2004.
- Ho, T.-Y., Taylor, G., Astor, Y., Varela, R., Taylor, G. T., and Scranton, M. I.: Vertical and temporal variability of redox zonation in the water column of the Cariaco: implications for organic carbon oxidation pathways, *Mar. Chem.*, 86, 89–104, 2004.
- Holmes, R. M., Aminot, A., Kérouel, R., Hooker, B. A., and Peterson, B. J.: A simple and precise method for measuring ammonium in marine and freshwater ecosystems, *Can. J. Fish. Aquat. Sci.*, 56, 1801–1808, 1999.
- IPCC.: *Climate Change: The Scientific Basis*, edited by: Houghton, J. T., Ding, Y., Griggs, D. J., Noguier, M., van der Linden, P. J., Dai, X., Maskell, K., and Johnson, C. A., Cambridge University Press, 2001.
- Janson, P. B. M., Malandrino, L., and Johansson, H.: Cell cycle arrest in Archea by the Hypusination inhibitor N^1 -Guanyl-1, 7-Diaminoheptane, *J. Bacteriol.*, 182, 1158–1161, 2000.
- Jørgensen, B. B. and Gallardo, V. A.: *Thioploca* spp.: Filamentous sulfur bacteria with nitrate vacuoles, *FEMS Microb. Ecol.*, 28, 301–313, 1999.
- Jost, G., Zubkov, M. V., Yakushev, E., Labrenz, M., and Jürgens, K.: High abundance and dark CO_2 fixation of chemolithotrophic prokaryotes in anoxic water of the Baltic Sea, *Limnol. Oceanogr.*, 53, 14–22, 2008.
- Joyce, S. B. and Hollibaugh, J. T.: Influence of sulfide inhibition of nitrification on nitrogen regeneration in sediments, *Science*, 270, 623–625, 1995.
- Labrenz, M., Jost, G., Pohl, C., Beckmann, S., Martens-Habbena, W., and Jürgens, K.: Impact of different in vitro Electron donor/acceptor conditions on potential chemolithoautotrophic communities from marine pelagic redoxclines, *Appl. Environ. Microb.*, 71, 6664–6672, 2005.
- Lavik, G., Stührmann, T., Brüchert, V., Van der Plas, A., Mohrholz, V., Lam, P., Mußmann, M., Fuchs, B. M., Amann, R., Lass, U., and Kuypers, M. M. M.: Detoxification of sulphidic African shelf waters by blooming chemolithotrophs, *Nature*, 457, 581–584, 2009.
- Law, C. S. and Owens, N. J. P.: Significance flux of atmospheric nitrous oxide from the northwest Indian Ocean, *Nature*, 346, 826–828, 1990.
- Lein, A. Y., Pimenov, N. V., and Galchenko, V. F.: Bacterial chemosynthesis and methanotrophy in the Manus and Lau basin ecosystems, *Mar. Geol.*, 142, 47–56, 1997.
- Levipan, H. A., Quiñones, R. A., and Urrutia, H.: A time series of prokaryote secondary production in the oxygen minimum zone of the Humboldt Current System, *Prog. Oceanogr.*, 75, 531–549, 2007a.
- Levipan, H. A., Quiñones, R. A., Johansson, H. E., and Urrutia, H.: Methylophilic Methanogens in the Water Column of an Upwelling Zone with a Strong Oxygen Gradient Off Central Chile, *Microb. Environ.*, 22, 268–278, 2007b.
- Madigan, M., Martinko, J., and Parker, J.: *Brock Biology of Microorganism. Nutrition and Metabolism*, Prentice Hall, New Jersey, 1011 pp., 2003.

- Naqvi, S. W. A., Jayakumar, D. A., Narvekar, P. V., Naik, H., Sarma, V. V., D'Souza, W., Joseph, S., and George, M. D.: Increased marine production of N₂O due to intensifying anoxia on the Indian continental shelf, *Nature*, 408, 346–349, 2000.
- Nevison, C. D., Weiss, R. F., and Erickson, D. J.: Global oceanic emissions of nitrous oxide, *J. Geophys. Res.*, 100, 15809–15820, 1995.
- Nevison, C. D., Lueker, T. J., and Weiss, R. F.: Quantifying the nitrous oxide source from coastal upwelling, *Global Biogeochem. Cy.*, 18, GB1018, doi:10.1029/2003GB002110, 2004.
- Owens, N. J. P., Law, C. S., Mantoura, R. F., Burkill, P. H., and Llewellyn, C. A.: Methane flux to the atmosphere from the Arabian Sea, *Nature*, 354, 293–296, 1991.
- Pauly, D. and Christensen, V.: Primary production required to sustain global fisheries, *Nature*, 374, 255–257, 1995.
- Pimenov, N. V. and Neretin, L.: Composition and activities of microbial communities involved in carbon, sulfur, nitrogen and manganese cycling in the oxic/anoxic interface of the Black Sea, edited by: Neretin, L. N., Past and present Water Column Anoxia. NATO Science Series: IV: Earth and Environmental Sciences, 501–502, 2006.
- Quiñones, R. A., Levipan, H. A., and Urrutia, H.: Spatial and temporal variability of planktonic archaeal abundance in the Humboldt Current System off Chile, *Deep Sea Res II.*, 56(16), 1073–1072, 2009.
- Rykaczewski, R. R. and Checkley Jr., D. M.: Influence of ocean winds on the pelagic ecosystem in upwelling regions, *Poner el nombre complete, P. Natl. Acad. Sci.*, 105, 1965–1970, doi:10.1073/pnas.0711777105, 2008.
- Schubert, C. J., Coolen, M. J. L., Neretin, N. L., and Schippers, A.: Aerobic and anaerobic methanotrophs in the Black Sea water column, *Environ. Microbiol.*, 8, 1844–1856, 2006.
- Sobarzo, M. and Djurfeldt, L.: Coastal upwelling process on a continental shelf limited by submarine canyons, Concepción, central Chile, *J. Geophys. Res.*, 109, C12012, doi:10.1029/2004JC002350, 2004.
- Slawyk, G. and Collos, Y.: ¹³C and ¹⁵N uptake by marine phytoplankton III. Interactions in euphotic zone profiles of stratified oceanic areas, *Mar. Ecol. Prog. Ser.*, 19, 223–231, 1984.
- Stramma, L., Johnson, G. C., Sprintall J., and Mohrholz, V.: Expanding Oxygen-Minimum Zones in the Tropical Oceans, *Science*, 320, 655–658, 2008.
- Strub, P. T., Mesías, J., Montecinos, V., Rutllant J., and Salinas, S.: Coastal ocean circulation off western south America, in: *The Sea*, edited by: Robinson A. R. and Brink, K. H, John Wiley & Sons, 273–313, 1998.
- Taylor, G. T., Iabichella, M., Tung-yuan, H., Scranton, M., Thunell, R., Muller-Karger, F., and Varela, R.: Chemoautotrophy in the redox transition zone of the Cariaco Basin: A significant midwater source of organic carbon production, *Limnol. Oceanogr.*, 46, 148–163, 2001.
- Thamdrup, B. and Canfield, D. E.: Pathway of carbon oxidation in the continental margin off central Chile, *Limnol. Oceanogr.*, 41, 1629–1650, 1996.
- Trotsenko, Y. A. and Murrell, J. C.: Metabolic aspects of aerobic obligate methanotrophy, *Adv. Appl. Microbiol.*, 63, 183–229, 2008.
- Upstill-Goddard, R. C., Barnes, J., and Owens, N. J.: Nitrous oxide and methane during the SW monsoon in the Arabian Sea/northwestern Indian Ocean, *J. Geophys. Res.*, 104, 30067–30084, 1999.
- Wanninkhof, R.: Relationship between wind speed and gas exchange over the ocean, *J. Geophys. Res.*, 97, 7373–7382, 1992.
- Ward, B. B., Glover, H. E., and Lipschultz, F.: Chemoautotrophic activity and nitrification in the oxygen minimum zone off Peru, *Deep Sea Res.*, 36, 1031–1051, 1989.
- Weisenburg, D. A. and Guinasso, N. L.: Equilibrium solubilities of methane, carbon monoxide and hydrogen in water and seawater, *J. Chem. Eng. Data*, 24, 354–360, 1979.
- Weiss, R. F. and Price, B. A.: Nitrous oxide solubility in water and seawater, *Mar. Chem.*, 8, 347–359, 1980.
- Zopfi, J., Ferdelman, T. G., Jorgensen, B. B., Teske, A., and Thamdrup, B.: Influence of water columns dynamics on sulfide oxidation and other major biogeochemical processes in the chemocline of Mariager Fjord (Denmark), *Mar. Chem.*, 74, 29–51, 2001.